Supporting Information

Ultrahigh spectral sensitivity of plasmon resonances in a nanocavity

Da-Jie Yang,[a,b] Shunping Zhang,[b] Song-Jin Im,[b,c] Qu-quan Wang,[*,b]

Hongxing Xu,[*,b] and Shiwu Gao[*,a]

[a] *Beijing Computational Science Research Center, 100193 Beijing, China. E-mail: swgao@csrc.ac.cn*

[b] *The Institute for Advanced Studies, School of Physics, Wuhan University, Wuhan, China. E-mail: qqwang@whu.edu.cn, hxxu@whu.edu.cn*

c *Department of Physics, Kim Il Sung University, Pyongyang, Democratic People's Republic of Korea*

1. Dispersion relation at infinite-length MIM' interfaces

We now focus on TM solutions of the infinite-length MIM' cavity shown in the left panel of Fig. S1. Assume that the material is nonmagnetic ($\mu_r = 1$), and that the solutions are superposition of single surfaces'.

For $-a < z < a$, (in the gap)

$$H_{1y} = (Ae^{-k_{1z}z} + Be^{k_{1z}z})e^{ik_x x} \quad (1a)$$

$$E_{1x} = (Ae^{-k_{1z}z} - Be^{k_{1z}z})\frac{ik_{1z}}{\omega\varepsilon_0\varepsilon_1}e^{ik_x x} \quad (1b)$$

$$E_{1z} = (Ae^{-k_{1z}z} + Be^{k_{1z}z})\frac{-k_x}{\omega\varepsilon_0\varepsilon_1}e^{ik_x x} \quad (1c)$$

and for $z > a$, (in metal I)

$$H_{3y} = (Ae^{-k_{1z}a} + Be^{k_{1z}a})\,\mathrm{e}^{-\mathrm{k}_{3z}(\mathrm{z}-\mathrm{a})}\,e^{ikx} \quad (2a)$$

$$E_{3x} = (Ae^{-k_{1z}a} + Be^{k_{1z}a})\frac{ik_{3z}}{\omega\varepsilon_0\varepsilon_3}\mathrm{e}^{-k_{3z}(z-a)}\,e^{ikx} \quad (2b)$$

$$E_{3z} = (Ae^{-k_{1z}a} + Be^{k_{1z}a})\frac{-k_x}{\omega\varepsilon_0\varepsilon_3}\mathrm{e}^{-k_{3z}(z-a)}\,e^{ikx} \quad (2c)$$

and for $z < -a$, (in metal II)

$$H_{2y} = (Ae^{k_{1z}a} + Be^{-k_{1z}a})\, e^{k_{2z}(z+a)}\, e^{ik_x x} \tag{3a}$$

$$E_{2x} = (Ae^{k_{1z}a} + Be^{-k_{1z}a})\, \frac{-ik_{2z}}{\omega\varepsilon_0\varepsilon_2}\, e^{k_{2z}(z+a)}\, e^{ik_x x} \tag{3b}$$

$$E_{2z} = (Ae^{k_{1z}a} + Be^{-k_{1z}a})\, \frac{-k_x}{\omega\varepsilon_0\varepsilon_2}\, e^{k_{2z}(z+a)}\, e^{ik_x x}. \tag{3c}$$

In Eqs. (1-3),

$$k_{1z}^2 = k_x^2 - \left(\frac{\omega}{c}\right)^2 \varepsilon_1 \tag{4a}$$

$$k_{2z}^2 = k_x^2 - \left(\frac{\omega}{c}\right)^2 \varepsilon_2 \tag{4b}$$

$$k_{3z}^2 = k_x^2 - \left(\frac{\omega}{c}\right)^2 \varepsilon_3 \tag{4c}$$

in which the subscriber i = 1, 2, 3 is corresponding to the region of $-a < z < a$, (within the cavity) $z < -a$ (in metal II) and $z > a$ (in metal I). Requirement of continuity of E_x at the interface leads to

$$(Ae^{-k_{1z}a} - Be^{k_{1z}a})\, \frac{ik_{1z}}{\omega\varepsilon_0\varepsilon_1}\, e^{ik_x x} = (Ae^{-k_{1z}a} + Be^{k_{1z}a})\, \frac{ik_{3z}}{\omega\varepsilon_0\varepsilon_3}\, e^{ik_x x} \quad (z = a) \tag{5a}$$

$$(Ae^{k_{1z}a} - Be^{-k_{1z}a})\, \frac{ik_{1z}}{\omega\varepsilon_0\varepsilon_1}\, e^{ik_x x} = (Ae^{k_{1z}a} + Be^{-k_{1z}a})\, \frac{-ik_{2z}}{\omega\varepsilon_0\varepsilon_2}\, e^{ik_x x} \quad (z = -a) \tag{5b}$$

Make a simplification, then we have

$$(Ae^{-k_{1z}a} - Be^{k_{1z}a})\, \frac{k_{1z}}{\varepsilon_1} = (Ae^{-k_{1z}a} + Be^{k_{1z}a})\, \frac{k_{3z}}{\varepsilon_3} \quad (z = a) \tag{6a}$$

$$(Ae^{k_{1z}a} - Be^{-k_{1z}a})\, \frac{k_{1z}}{\varepsilon_1} = (Ae^{k_{1z}a} + Be^{-k_{1z}a})\, \frac{-k_{2z}}{\varepsilon_2} \quad (z = -a) \tag{6b}$$

We can get the specific values of B and A from Eq. (6)

$$\frac{B}{A} = \frac{k_{1z}\varepsilon_3 - k_{3z}\varepsilon_1}{k_{1z}\varepsilon_3 + k_{3z}\varepsilon_1}\, e^{-2k_{1z}a} \quad (z = a) \tag{7a}$$

$$\frac{B}{A} = \frac{k_{1z}\varepsilon_2 + k_{2z}\varepsilon_1}{k_{1z}\varepsilon_2 - k_{2z}\varepsilon_1}\, e^{2k_{1z}a} \quad (z = -a) \tag{7b}$$

If the TM solutions exists, the specific values of B and A from Eqs. (7a) and (7b) should be the same. From these two equations we have

$$e^{-4k_{1z}a} = \frac{k_{1z}\varepsilon_2 + k_{2z}\varepsilon_1}{k_{1z}\varepsilon_2 - k_{2z}\varepsilon_1}\, \frac{k_{1z}\varepsilon_3 + k_{3z}\varepsilon_1}{k_{1z}\varepsilon_3 - k_{3z}\varepsilon_1}. \tag{8}$$

Eq. (8) is the disperse relation of the MIM' system.

In the special case of symmetric MIM cavity ($\varepsilon_2 = \varepsilon_3$), the disperse relation will become

$$\frac{k_{1z}\varepsilon_2 - k_{2z}\varepsilon_1}{k_{1z}\varepsilon_2 + k_{2z}\varepsilon_1} = \pm e^{2k_{1z}a}. \quad (9)$$

① When $\frac{k_{1z}\varepsilon_2 - k_{2z}\varepsilon_1}{k_{1z}\varepsilon_2 + k_{2z}\varepsilon_1} = e^{2k_{1z}a}$, that is $k_{1z}\varepsilon_2 + k_{2z}\varepsilon_1 < 0$, or

$\left|k_{1z} / \varepsilon_1\right| > \left|k_{2z} / \varepsilon_2\right|$,

$$e^{k_{1z}a} = \left(\frac{k_{1z}\varepsilon_2 - k_{2z}\varepsilon_1}{k_{1z}\varepsilon_2 + k_{2z}\varepsilon_1}\right)^{\frac{1}{2}} \quad (10)$$

$$e^{-k_{1z}a} = \left(\frac{k_{1z}\varepsilon_2 + k_{2z}\varepsilon_1}{k_{1z}\varepsilon_2 - k_{2z}\varepsilon_1}\right)^{\frac{1}{2}} \quad (11)$$

$$\tanh(k_{1z}a) = \frac{e^{k_{1z}a} - e^{-k_{1z}a}}{e^{k_{1z}a} + e^{-k_{1z}a}} = -\frac{k_{2z}\varepsilon_1}{k_{1z}\varepsilon_2}. \quad (12)$$

Now we have B/A = 1.
Insert this value to Eq. (1), we can find $E_x(z)$ is odd function, and that $H_y(z)$ and $E_z(z)$ are even functions.[1]

② When $\frac{k_{1z}\varepsilon_2 - k_{2z}\varepsilon_1}{k_{1z}\varepsilon_2 + k_{2z}\varepsilon_1} = -e^{2k_{1z}a}$, that is $k_{1z}\varepsilon_2 + k_{2z}\varepsilon_1 > 0$, or

$\left|k_{1z} / \varepsilon_1\right| < \left|k_{2z} / \varepsilon_2\right|$,

$$e^{k_{1z}a} = \left(\frac{k_{2z}\varepsilon_1 - k_{1z}\varepsilon_2}{k_{1z}\varepsilon_2 + k_{2z}\varepsilon_1}\right)^{\frac{1}{2}} \quad (13)$$

$$e^{-k_{1z}a} = \left(\frac{k_{1z}\varepsilon_2 + k_{2z}\varepsilon_1}{k_{2z}\varepsilon_1 - k_{1z}\varepsilon_2}\right)^{\frac{1}{2}} \quad (14)$$

$$\tanh(k_{1z}a) = -\frac{k_{1z}\varepsilon_2}{k_{2z}\varepsilon_1}. \quad (15)$$

Now we have B/A = -1.
Insert this value to Eq. (1), we can find $E_x(z)$ is even functions, and that $H_y(z)$ and $E_z(z)$ are odd functions.[1]

2. Resonance condition at finite-length MIM' interfaces

We now consider the solution of MIM' interfaces with finite metal side lengths shown in Fig. S2. The side lengths of the cuboid in the x and y directions are L_x, L_y and the gap size is $2a$.
When the electromagnetic wave propagates along the small gap, standing wave will form because

of the reflection at the boundaries of the cavity. This mode is the so-called cavity plasmon mode. According to Fabry-Pérot conditions, resonance condition should be

$$\begin{cases} k_x = \dfrac{m\pi}{L_x} & (\mathrm{m} = 0, 1, 2 \ldots) \\ k_y = \dfrac{n\pi}{L_y} & (n = 0, 1, 2 \ldots) \end{cases} \tag{2.1}$$

Differently, as a consequence of the aperture effect, the resonance peaks of the finite-length MIM cavity will have a symmetric shift towards longer wavelength.[2,3] The reason is that a phase shift occurs when the electromagnetic field is reflected at the boundary. The resonance condition becomes

$$k_x L_x + \Delta\varphi = m\pi \tag{2.2a}$$

$$k_y L_y + \Delta\varphi = n\pi \tag{2.2b}$$

The expression of the phase shift $\Delta\varphi$ is detailed discussed below. Then we have

$$k_x = \frac{m\pi - \Delta\varphi}{L_x} \tag{2.3a}$$

$$k_y = \frac{n\pi - \Delta\varphi}{L_y} \tag{2.3b}$$

Insert resonance condition Eq. (2.3) into dispersion relation Eq. (12), and combine the wave vector relation Eq. (4), we will have the resonance wavelength of different modes and the corresponding field distribution.

$$E_z^{\mathrm{cav}} = \sum_{m=0}^{\infty}\sum_{n=0}^{\infty} E_{1mn} \sin(k_x x)\sin(k_y y)(Ae^{-ik_{1z}z} + Be^{ik_{1z}z}) \tag{2.4}$$

The electric field of different TM modes are shown in Fig. S3.

3. Simplification and approximation

Surely, we can get the resonance wavelength by combining Eq. (20), (12), and (4). We want to make the equations clearer to see the influence of geometry and the materials. We can also make further approximation to get more physical results by handling the dispersion relation. There will be two approximations during the problem-solving process. First when the gap size $2a$ approaches zero and $\varepsilon_2 \gg \varepsilon_1$, for the MIM interface, $k_{1z}\varepsilon_2 \gg k_{2z}\varepsilon_1$ and $2k_{1z}a \to 0$, which can be reflected from Fig. S4a. So Eq. (12) can be simplified as

$$1 + \frac{2k_{2z}\varepsilon_1}{k_{1z}\varepsilon_2} = 1 - 2k_{1z}a \tag{3.1}$$

That is

$$\frac{k_{2z}\varepsilon_1}{k_{1z}\varepsilon_2} = -k_{1z}a \tag{3.2}$$

The dispersion relation become simpler with Eq. (3.2). Combine Eq. (3.2) with the wave vector relation Eq. (4), we will have the resonance wavelength. Results before and after this approximation are shown in Fig. S4b. The good agreements prove the rationality of this approximation.
Transform Eq. (3.2), we will have

$$k_{1z}^2 = -\frac{k_{2z}\varepsilon_1}{a\varepsilon_2} \qquad (3.3)$$

Put Eq. (3.3) into the wave vector relation Eq. (4a), we will have

$$-\frac{k_{2z}\varepsilon_1}{a\varepsilon_2} = k_x^2 - \left(\frac{\omega}{c}\right)^2 \varepsilon_1 \qquad (3.4)$$

Make a transformation, we will have

$$k_{2z} = -\frac{a\varepsilon_2}{\varepsilon_1}\left(k_x^2 - \left(\frac{\omega}{c}\right)^2 \varepsilon_1\right) \qquad (3.5)$$

Put Eq. (3.5) into wave vector relation Eq. (4b), we will have

$$\left(\frac{a\varepsilon_2}{\varepsilon_1}\right)^2 \left(k_x^2 - \left(\frac{\omega}{c}\right)^2 \varepsilon_0\right)^2 = k_x^2 - \left(\frac{\omega}{c}\right)^2 \varepsilon_2 \qquad (3.6)$$

Solve Eq. (3.6), we will have

$$\left(\frac{\omega}{c}\right) = \frac{1}{\sqrt{2}}\sqrt{\left|\frac{2k_x^2}{\varepsilon_1} - \frac{1}{a^2\varepsilon_2} + \frac{1}{a^2\varepsilon_2}\sqrt{1+4k_x^2a^2\left(1-\frac{\varepsilon_2}{\varepsilon_1}\right)}\right|} \qquad (3.7)$$

Then the second approximation will be made here to simplify the equation. When the gap size $2a$ approaches zero for the MIM interface, $2k_{1z}a \to 0$. Then

$$\frac{1}{a^2\varepsilon_2}\sqrt{1+4k_x^2a^2\left(1-\frac{\varepsilon_2}{\varepsilon_1}\right)} \approx \frac{1}{a^2\varepsilon_2}\left(1+2k_x^2a^2\left(1-\frac{\varepsilon_2}{\varepsilon_1}\right) - \frac{1}{8}\left(4k_x^2a^2\left(1-\frac{\varepsilon_2}{\varepsilon_1}\right)\right)^2\right) \qquad (3.8)$$

Put Eq. (3.8) onto Eq. (3.7), we have

$$\left(\frac{\omega}{c}\right) = \frac{k_x}{\sqrt{\varepsilon_2}}\sqrt{1-k_x^2a^2\left(1-\frac{\varepsilon_2}{\varepsilon_1}\right)^2} \qquad (3.9)$$

The influence of the second approximation is shown in Fig. S4b. We can find the second approximation indeed bring somewhat errors. If we added the fourth item into Eq. (3.6), the result becomes better, but the output will become complex. So we deny to add the fourth item. Finally, after two approximations, the resonance wavelength of the MIM cavity is

$$\lambda = \frac{2\pi c}{\omega} \qquad (3.10)$$

$$= \frac{2\pi\sqrt{\varepsilon_2}}{k_x\sqrt{1-k_x^2a^2\left(1-\frac{\varepsilon_2}{\varepsilon_1}\right)^2}} \qquad (3.11)$$

Combine Eq. (3.11) with the resonance condition Eq. (2.3), we will have the resonance wavelength of the finite MIM cavity. The equations become much simpler with these two rational approximations.

4. Phase shift

Phase shift occurs when electromagnetic field is reflected at the boundary. This can be determined by the complex reflection coefficient *r*. Two boundary conditions are needed to calculated *r*, that is the continuity of the electromagnetic field and the continuity of the total Poynting flux.[5,6] So we have

$$\left(1 + r\right) E_z = E_z^{\mathrm{fs}} \qquad (4.1)$$

$$\left(1 - r\right) H_y = H_y^{\mathrm{fs}} \qquad (4.2)$$

$$\int S_x^{\mathrm{cav}} dz = \int S_x^{\mathrm{fs}} dz \qquad (4.3)$$

in which, superscripts "cav" and "fs" are corresponding to the quantities corresponding to SPP electromagnetic field and the electromagnetic field transmitting into the free space. Combining Eq. (4.1-4.3), we have

$$\left(1 + r\right)\left(1 - r^*\right) \int E_z H_y^* dz = \int E_z^{\mathrm{fs}} H_y^{\mathrm{fs}*} dz \qquad (4.4)$$

The Fourier transformation of the electric field in the free space can be written as

$$\begin{aligned} E_z^{\mathrm{fs}} &= \int f(k_z) e^{ik_z z} dk_z \\ &= \int \left(\frac{1 + r}{2\pi} \int E_z e^{-ik_z z} dz \right) e^{ik_z z} dk_z \\ &= \int \left(\frac{1 + r}{2\pi} I(k_z) \right) e^{ik_z z} dk_z \qquad (4.5) \end{aligned}$$

in which

$$I(k_z) = \int E_z e^{-ik_z z} dz \qquad (4.6)$$

The magnetic field in the free space, H_y^{fs}, can be obtained according to Faraday's Law

$$H_y^{\mathrm{fs}} = \frac{1}{i\omega\mu_0} \left(\frac{\partial E_x^{fs}}{\partial z} - \frac{\partial E_z^{fs}}{\partial x} \right) \qquad (4.7)$$

$\frac{\partial E_x^{fs}}{\partial z}$ and $\frac{\partial E_z^{fs}}{\partial x}$ can be expressed as

$$\frac{\partial E_x^{\mathrm{fs}}}{\partial z} = \frac{ik_{1z}^2}{k_x} E_z^{fs} \qquad (4.8)$$

$$\frac{\partial E_z^{\mathrm{fs}}}{\partial x} = ik_x E_z^{fs} \qquad (4.9)$$

Put Eqs. (4.8, 4,9) into Eq. (4.7), and substitute k_{1z}^2 with $-k_z^2$, we will have

$$H_y^{\mathrm{fs}} = \frac{-1}{\omega\mu_0}\frac{1+r}{2\pi}\int I(k_z)\frac{\varepsilon_1 k_0^2}{\sqrt{\varepsilon_1 k_0^2 - k_z^2}} e^{ik_z z} dk_z \qquad (4.10)$$

Put Eq. (4.5, 4.10) into the right part of Eq. (4.4), we have

$$\begin{aligned}
\int E_z^{\mathrm{fs}} H_y^{\mathrm{fs}*} dz &= -\frac{(1+r)(1+r^*)}{\omega\mu_0 2\pi \cdot 2\pi}\int\left[\int I(k_z{}')e^{ik_z' z}dk_z{}'\right]\left[\int \frac{I(k_z)\varepsilon_1 k_0^2}{\sqrt{\varepsilon_1 k_0^2 - k_z^2}} e^{ik_z z}dk_z\right]dz \\
&= -\frac{(1+r)(1+r^*)}{\omega\mu_0 2\pi \cdot 2\pi}\iint I(k_z{}')\frac{I(k_z)\varepsilon_1 k_0^2}{\sqrt{\varepsilon_1 k_0^2 - k_z^2}}\left[\int e^{i(k_z - k_z{}')z}dz\right]dk_z{}'dk_z \\
&= -\frac{(1+r)(1+r^*)}{\omega\mu_0 2\pi}\iint I(k_z{}')\frac{I(k_z)\varepsilon_1 k_0^2}{\sqrt{\varepsilon_1 k_0^2 - k_z^2}}\delta(k_z - k_z{}')dk_z{}'dk_z \\
&= -\frac{(1+r)(1+r^*)}{\omega\mu_0 2\pi}\int \frac{I(k_z)\varepsilon_1 k_0^2}{\sqrt{\varepsilon_1 k_0^2 - k_z^2}}\left[\int I(k_z{}')\delta(k_z - k_z{}')dk_z{}'\right]dk_z \\
&= -\frac{(1+r)(1+r^*)}{\omega\mu_0 2\pi}\int \frac{I(k_z)\varepsilon_1 k_0^2}{\sqrt{\varepsilon_1 k_0^2 - k_z^2}} I(k_z)dk_z \\
&= -\frac{(1+r)(1+r^*)}{\omega\mu_0 2\pi}\int \frac{|I(k_z)|^2\,\varepsilon_1 k_0^2}{\sqrt{\varepsilon_1 k_0^2 - k_z^2}}dk_z \qquad (4.11)
\end{aligned}$$

Put Eq. (4.11) into Eq. (4.4) and make a simplification, we will have

$$\begin{aligned}
\frac{(1-r^*)}{(1+r^*)} &= \frac{1}{\omega\mu_0 2\pi/k_0^2}\frac{1}{\int E_z H_y^* dz}\int \frac{-|I|^2\,\varepsilon_1}{\sqrt{\varepsilon_1 k_0^2 - k_z^2}} e^{ik_z z}dk_z \\
&= \frac{1}{\lambda Z_0}\frac{1}{\int E_z H_y^* dz}\int \frac{-|I|^2\,\varepsilon_1}{\sqrt{\varepsilon_1 k_0^2 - k_z^2}} e^{ik_z z}dk_z \qquad (4.12)
\end{aligned}$$

Assuming that

$$G = \frac{1}{\lambda Z_0}\frac{1}{\int E_z H_y^* dz}\int \frac{-|I|^2\,\varepsilon_1}{\sqrt{\varepsilon_1 k_0^2 - k_z^2}} e^{ik_z z}dk_z \qquad (4.13),$$

we have

$$r = \left(\frac{1-G}{1+G}\right)^* \qquad (4.14)$$

Finally, the phase shift can be written as

$$\triangle\varphi = \arctan\left(\frac{r_1}{r_2}\right) \qquad (4.15)$$

where r_1 and r_2 are the real and imaginary parts of r respectively.

5. Nonlocal effect

1) Analytical model

Considering the nonlocal effect, the electric field and the magnetic field will be written as:[7]

For $-a < z < a$, (in the gap)

$$H_{1y} = (Ae^{-k_{1z}z} + Be^{k_{1z}z})e^{ik_x x} \tag{5. 1a}$$

$$E_{1x} = (Ae^{-k_{1z}z} - Be^{k_{1z}z})\frac{ik_{1z}}{\omega\varepsilon_0\varepsilon_1}e^{ik_x x} \tag{5. 1b}$$

$$E_{1z} = (Ae^{-k_{1z}z} + Be^{k_{1z}z})\frac{-k_x}{\omega\varepsilon_0\varepsilon_1}e^{ik_x x} \tag{5. 1c}$$

and for $z < -a$, (in metal)

$$H_{2y} = C\,\mathrm{e}^{k_{2z}(z+a)}\,e^{ik_x x} \tag{5. 2a}$$

$$E_{2x} = \left(C\frac{k_{2z}}{i\omega\varepsilon_0\varepsilon_2}\mathrm{e}^{k_{2z}(z+a)} + D\,\mathrm{e}^{\kappa_l(z+a)}\right)e^{ik_x x} \tag{5. 2b}$$

$$E_{2z} = \left(C\frac{-k_x}{\omega\varepsilon_0\varepsilon_2}\mathrm{e}^{k_{2z}(z+a)} + D\frac{\kappa_l}{ik_x}\mathrm{e}^{\kappa_l(z+a)}\right)e^{ik_x x}. \tag{5. 2c}$$

and for $z > a$, (in metal)

$$H_{2y} = C\,\mathrm{e}^{k_{2z}(z-a)}\,e^{ik_x x} \tag{5. 3a}$$

$$E_{2x} = \left(C\frac{k_{2z}}{i\omega\varepsilon_0\varepsilon_2}\mathrm{e}^{k_{2z}(z-a)} + D\,\mathrm{e}^{\kappa_l(z-a)}\right)e^{ik_x x} \tag{5. 3b}$$

$$E_{2z} = \left(C\frac{-k_x}{\omega\varepsilon_0\varepsilon_2}\mathrm{e}^{k_{2z}(z-a)} + D\frac{\kappa_l}{ik_x}\mathrm{e}^{\kappa_l(z-a)}\right)e^{ik_x x}. \tag{5. 3c}$$

In Eqs. (5.1-5.3),

$$k_{1z}^2 = k_x^2 - \left(\frac{\omega}{c}\right)^2\varepsilon_1 \tag{5. 4a}$$

$$k_{2z}^2 = k_x^2 - \left(\frac{\omega}{c}\right)^2\varepsilon_2 \tag{5. 4b}$$

$$\kappa_l^2 = k_x^2 + \frac{1}{\beta^2}\left(\omega^2 + i\gamma\omega - \frac{\omega_p^2}{\varepsilon_\infty}\right) \tag{5. 4c}$$

In Eqs. (5.1-5.4), A B C D are related to the coefficients of the incident wave, reflected wave, the transmission of the transverse wave and the transmission of the longitudinal wave. The longitudinal electromagnetic wave is induced by the nonlocal effect of the free electron. β is proportional to fermi vector and expressed as $\beta = \sqrt{\frac{3}{5}} v_F = \sqrt{\frac{3}{5}} \times 1.39 \times 10^6 \text{ m/s}$.

Requirement of continuity of E_x and H_y at the interface (z = - a) leads to

$$Ae^{k_{1z}a} + Be^{-k_{1z}a} = C \quad (5.6a)$$

$$(Ae^{-k_{1z}a} - Be^{k_{1z}a}) \frac{k_{1z}}{-i\omega\varepsilon_0\varepsilon_1} = C \frac{k_{2z}}{i\omega\varepsilon_0\varepsilon_2} + D \quad (5.6b)$$

And additional boundary conditions (ABCs) $\mathrm{P}_{fz} = \frac{1}{-i\omega}\frac{\partial H_y}{\partial x} - \varepsilon_0\varepsilon_\infty E_z = 0$ yields

$$ik_x C\left(\frac{1}{\varepsilon_2} - \frac{1}{\varepsilon_\infty}\right) = \frac{\kappa_l}{ik_x} i\omega\varepsilon_0 D \quad (5.6c)$$

Solve Eqs. (5.6), we will have

$$\frac{Ae^{k_{1z}a}}{Be^{-k_{1z}a}} = \frac{\frac{k_{1z}}{\varepsilon_1} - \frac{k_{2z}}{\varepsilon_2} + \Omega}{\frac{k_{1z}}{\varepsilon_1} + \frac{k_{2z}}{\varepsilon_2} - \Omega} \quad (5.7a)$$

In the similar way, at the interface (z = - a), we will have

$$\frac{Be^{k_{1z}a}}{Ae^{-k_{1z}a}} = \frac{\frac{k_{1z}}{\varepsilon_1} - \frac{k_{2z}}{\varepsilon_2} + \Omega}{\frac{k_{1z}}{\varepsilon_1} + \frac{k_{2z}}{\varepsilon_2} - \Omega} \quad (5.7b)$$

In which $\Omega = \frac{k_x^2}{\kappa_l}\left(\frac{1}{\varepsilon_2} - \frac{1}{\varepsilon_\infty}\right)$

Combine Eq. (5.7a) and (5.7b), and consider the symmetric mode ($C = D$), we will have the dispersion relation[7]

$$\tanh(k_{1z}a) = -\frac{k_{2z}\varepsilon_1}{k_{1z}\varepsilon_2} + \frac{k_{2z}\Omega}{k_{1z}}. \quad (5.8)$$

Combining dispersion Eq. 5.8 with the resonance condition Eq. 2.3, we can get the resonance wavelength allowing for the nonlocal effect.

2) Numerical implement of the nonlocal effect

Nonlocal effect become more significant when the gap reduces to sub-nanometer. The nonlocal effect will push the electrons at the surface into the metals. It has been proved that the nonlocal effect can be interpreted as a variation effective insulator thickness between the two cubes.[7-9] The gap width will be enlarged by Δd. Δd will be different according to different materials and boundary conditions for the free electrons. Here, we take $\Delta d = 0.08$ nm and reproduces the analytical results perfectly.

6. Comparison with the experiment results

The sensitivity found in the work is much larger than our experimental results (Nat. Commun. 2018, 9:801), simply because the side lengths and the gap widths are different.

1. In the experiment, the side length is about 43 nm, and it is smaller than that used in our analytical model. In Fig. 4 in the manuscript, the influence of the cavity length is shown, and the results show the sensitivity is strongly dependent on the cavity side length. So with much larger side length in our manuscript, it is reasonable to get larger sensitivity than our experiment data.
2. There is a radius at each corner of the nanowire in the experiment. The rounding reduces the sensitivity severely.
3. In the experiment, 0.5-nm-thick CTAB-covered Au-NWOM systems is separated by an Al2O3 film with thickness ranging from 5 to 0.5 nm. Due to the mirror effect, the efficient gap width will be doubled. So the cavity in the experiment is 2-10 nm, which is larger than 1 nm in our analytical model.
4. It is possible to reproduce the experimental result with the analytical model as well as the FEM simulations with proper choice of parameters, as shown in Fig. S7. The theoretical results agree well with the experimental results.

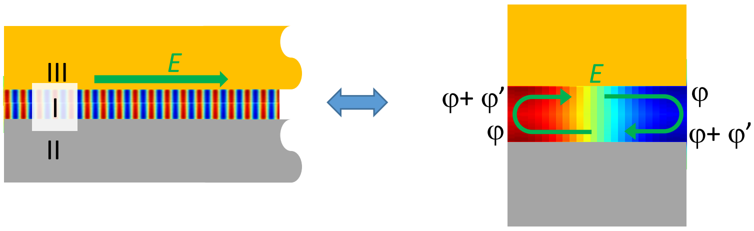

Fig. S1 Schematic of the SPP in an infinite-length MIM' cavity and localized cavity mode in a finite-length MIM' cavity. Light propagating along the infinite-length cavity will induce the propagating cavity surface plasmon mode, while light being reflected at finite-length cavity will generate localized cavity surface plasmon mode.

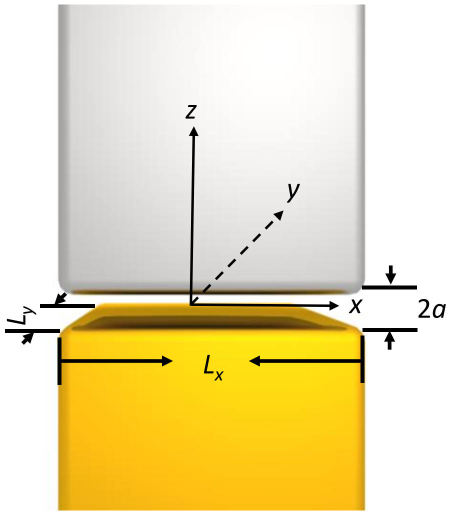

Fig. S2. Geometry for finite-length MIM' cavity when the side lengths in the x and y directions are L_x, L_y and the gap size is $2a$. The coordinate zero point is chosen at the middle of the gap.

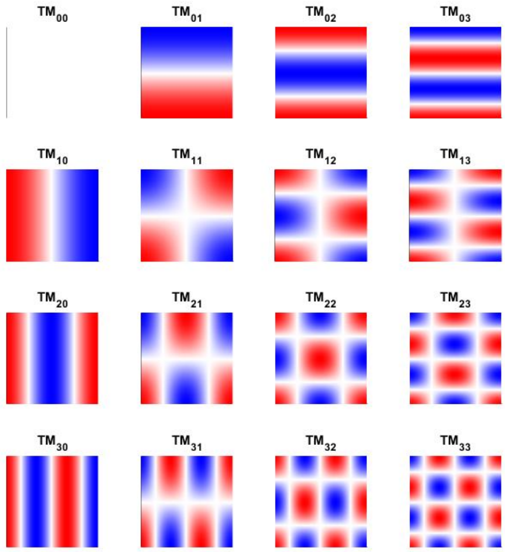

Fig. S3. Charge distributions of different TM modes at the interface of the insulator and one cube.

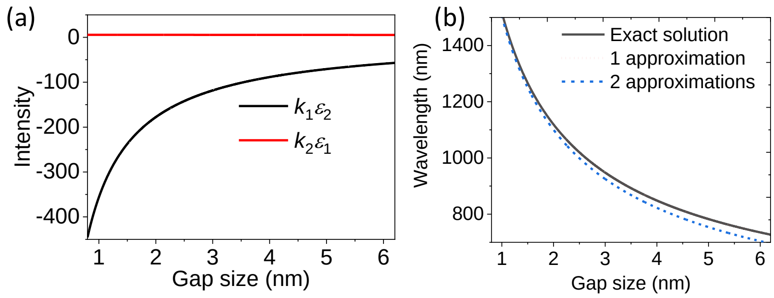

Fig. S4 (a) $k_{1z}\varepsilon_2$ and $k_{2z}\varepsilon_1$ as a function of the gap size $2a$. (b) Influence of the two approximations during the direct method.

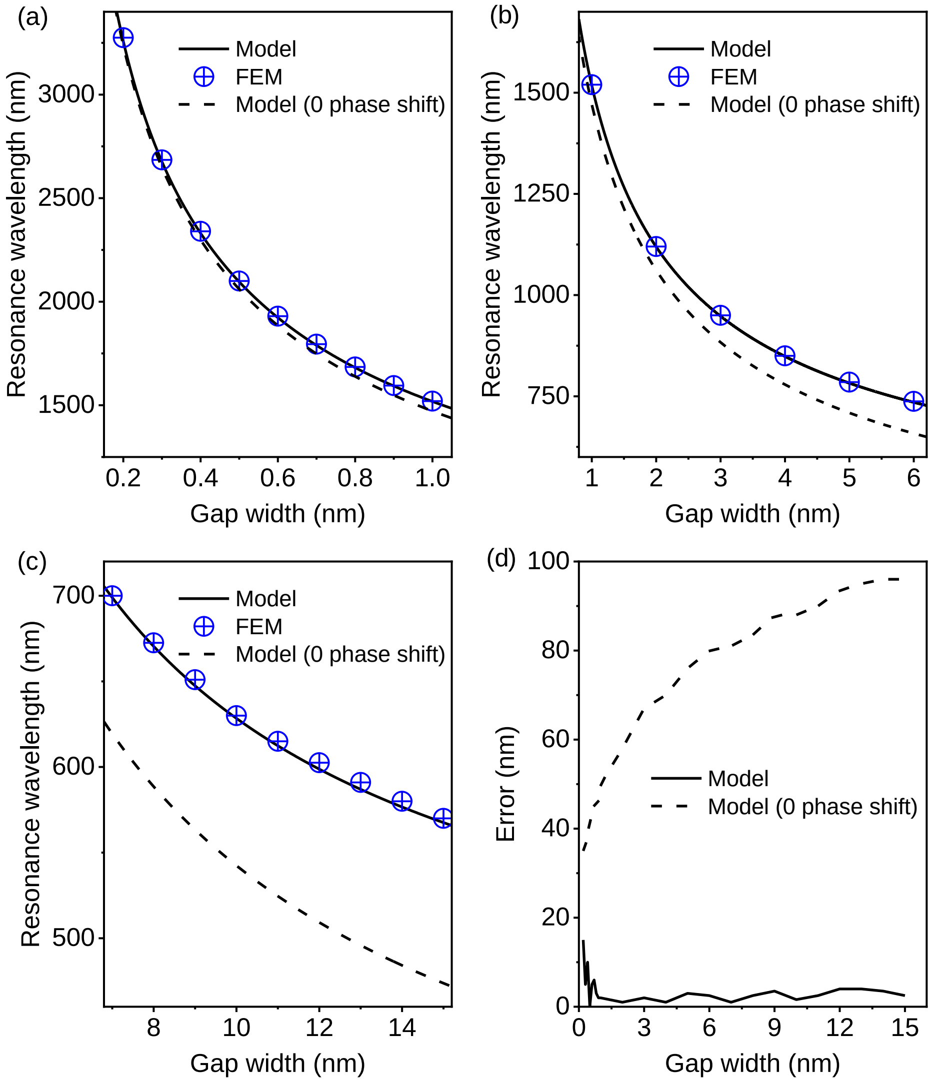

Fig. S5 Comparison of the analytical model considering (solid line) and neglecting (dash line) the phase shift at the boundary of the cavity with the FEM results (cross in circle). (a-c) show the resonance wavelength from different methods at different gap width ranges. (d) shows the errors (λ_{FEM} - λ_{Model}). The FEM simulation is performed in two dimensions (homogeneous in the $L_y = \infty$, and $L_x = L_z = 100$ nm). With the phase correction, the largest error is (15 nm/3000 nm = 0.5‰) when the gap width is 0.2 nm.

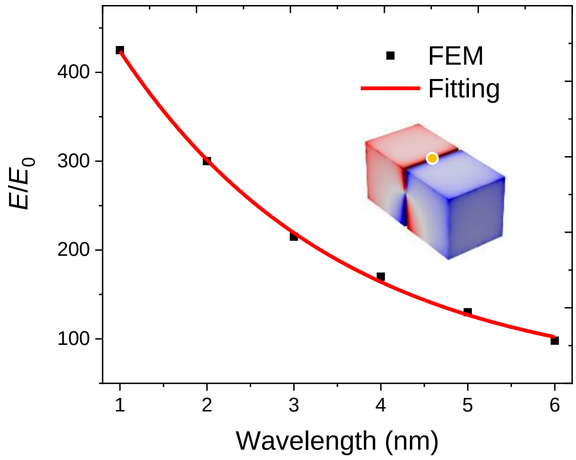

Fig. S6 Near field enhancement for different gap widths. *E* is the electric field collected at the position as show by the yellow dot in the inset.

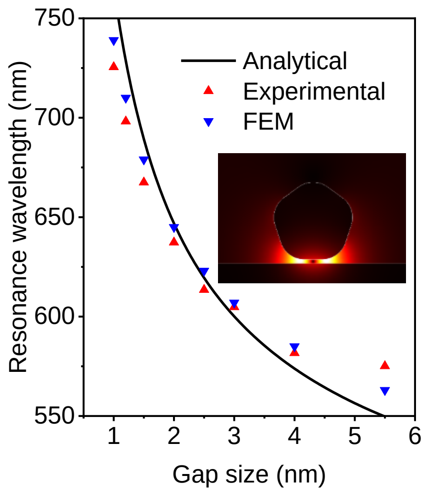

Fig. S7 Comparison of analytical model (lines), our prevously reported experimental data38 (up triangle) and FEM simulations (down triangule) of TM_{10} mode for gold NWOM. For the FEM simulations, the side-length of the nanowire is set to be 26.5 nm and its corners are rounded with a radius of 12 nm. Considering the interfaces of NWOM structure are not perfect, the refractive index of the dielectric spacer is set to be 1.3. Due to the mirror effect, the gap sizes are doubled in the analytical calculations. In the experiment, there is a molecule layer (0.5 nm), so we added this factor in the experiment results. These choices are reasonable because the rounded edges have multiple influences: decreasing the efficient side length and increasing the efficient gap size. We find good agreement between the theoretical calculations and the experiments, which once proves the validity of our analytical model.

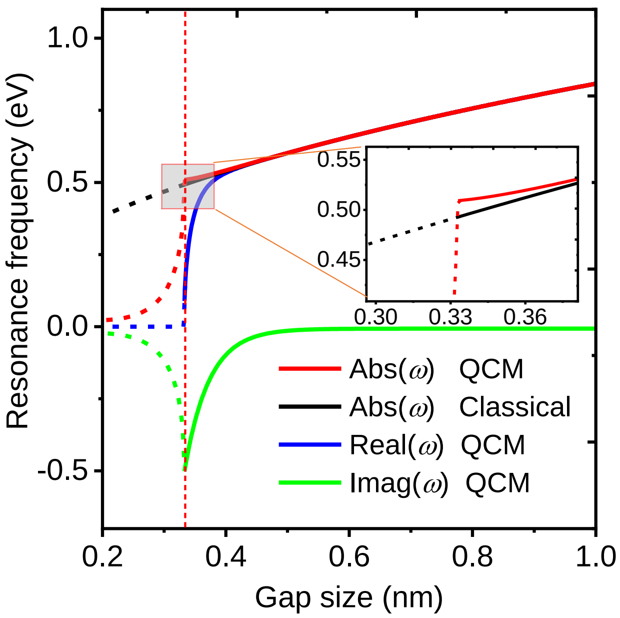

Fig. S8 Resonance frequency of the cavity plasmon mode as a function of the gap size considering (red line) and without considering (black line) the tunnelling effect. The blue and the green lines are the real and imaginary part of the solutions. Imaginary solution means the physically meaningful solutions doesn’t exist.

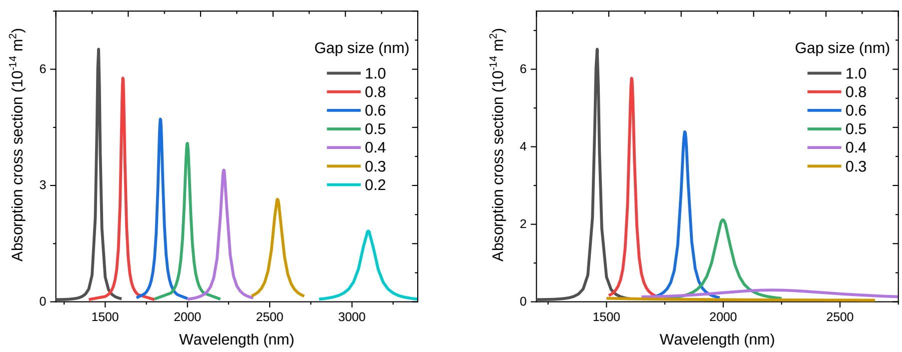

Fig. S9 FEM simulation of the absorption spectra by considering (a) and neglecting (b) the quantum tunneling effect. The cavity is a dimer of silver cubes whose side lengths are 100 nm.

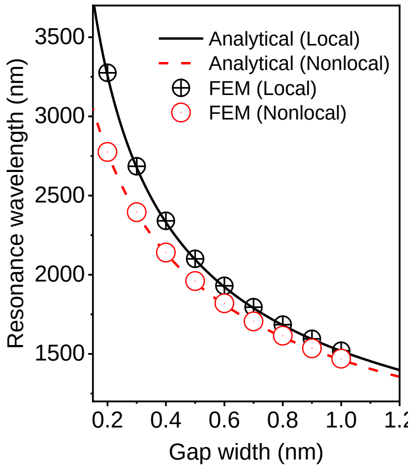

Fig. S10 Resonance wavelengths with and without nonlocal effect. In the analytical model, nonlocal effect is introduced by applying the dispersion of Eq. 5.8 in the ESI. In the FEM simulation, the nonlocal effect is introduced by replace the gap width *d* with *d* + Δ*d*, and Δ*d* = 0.08 nm.

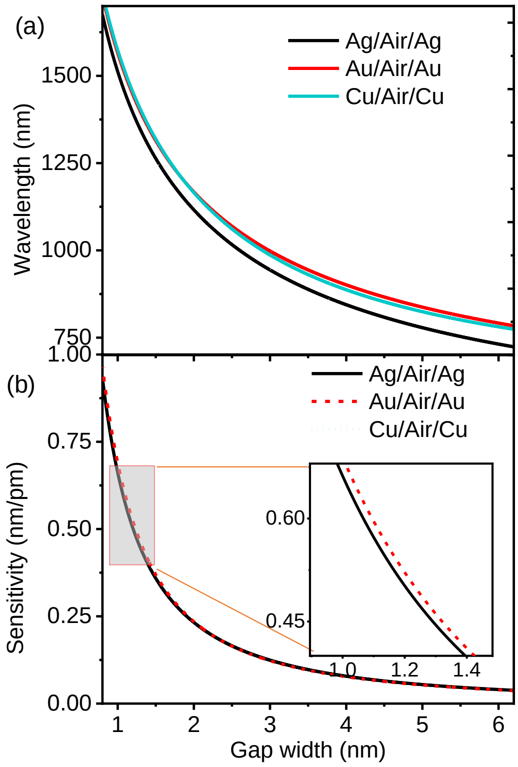

Fig. S11 Resonance wavelengths (a) and sensitivities (b) of Ag/air/Ag, Au/air/Au, and Cu/air/Cu cavities from the analytical model. The cavity lengths are 100 nm, and the refractive indices of the metals are from the experimental data of Ref. 11.

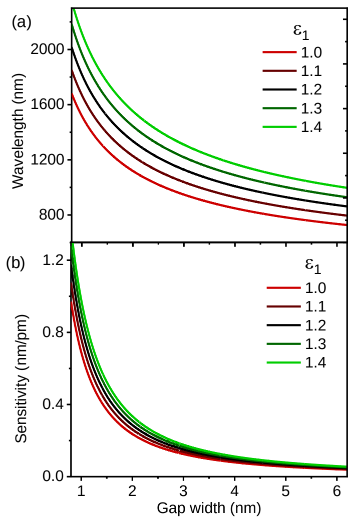

Fig. S12 Resonance wavelengths (a) and sensitivities (b) of TM_{10} mode of Ag/air/Ag cavity with different refractive indices of the media from the analytical model. The cavity lengths are 100 nm.

References

1. Maier, S. A. *Plasmonics*: *Fundamentals and Applications*; Springer, 2007.
2. Takakura, Y. Optical resonance in a narrow slit in a thick metallic screen. *Phys. Rev. Lett*. **2001**, *86*, 5601–5603.
3. Yang, F.; Sambles, J. R. Resonant Transmission of Microwaves through a Narrow Metallic Slit. *Phys. Rev. Lett*. **2002**, *89*, 063901.
4. Yang, J.; Sauvan, C.; Jouanin, A.; Collin, S.; Pelouard, J. L.; Lalanne, P. Ultrasmall metal-insulator-metal nanoresonators: impact of slow-wave effects on the quality factor. *Opt. Express*, **2012**, 20, 16880-16891.
5. Gordon R. Light in a subwavelength slit in a metal: propagation and reflection[J]. Physical Review B, 2006, 73(15): 153405.
6. Chandran A, Barnard E S, White J S, et al. Metal-dielectric-metal surface plasmon-polariton resonators[J]. Physical Review B, 2012, 85(8): 085416.
7. A. Moreau, C. Ciraci, D. R. Smith. Impact of nonlocal response on metallodielectric multilayers and optical patch antennas. Phys. Rev. B, 2013, 87(4): 045401.
8. Y. Luo, A. I. Fernandez-Dominguez, A. Wiener, S. A. Maier, J. B. Pendry. Surface plasmons and nonlocality: a simple model. Phys. Rev. Lett., 2013, 111(9): 093901.
9. R. Esteban, A. Zugarramurdi, P. Zhang, P. Nordlander, F. J. Garcia-Vidal, A. G. Borisov and J. Aizpurua, A classical treatment of optical tunneling in plasmonic gaps: extending the quantum corrected model to practical situations. Faraday Discuss., 2015, 178, 151–83.
10. W. Chen, S. Zhang, Q. Deng and H. Xu. Probing of sub-picometer vertical differential resolutions using cavity plasmons Nat. Commun., 2018, 9, 801
11. P. Johnson and R. Christy, Optical constants of transition metals: Ti, V, Cr, Mn, Fe, Co, Ni, and Pd. Phys. Rev. B, 1974, 9, 5056–5070.